Surface Science 603 (2009) 3094–3098

Contents lists available at ScienceDirect

Surface Science

journal homepage: www.elsevier.com/locate/susc

Adsorption of PTCDI on Au(1 1 1): Photoemission and scanning tunnelling microscopy

James N. O'Shea [a,*], Alex Saywell [a], Graziano Magnano [a], Luís M.A. Perdigão [a], Christopher J. Satterley [a], Peter H. Beton [a], Vinod R. Dhanak [b]

[a] School of Physics and Astronomy, University of Nottingham, Nottingham NG7 2RD, UK
[b] Surface Science Research Centre, University of Liverpool, UK

ARTICLE INFO

Article history:
Received 6 July 2009
Accepted for publication 21 August 2009
Available online 29 August 2009

Keywords:
Chemisorption
Aromatics
Scanning tunnelling microscopy
X-ray photoelectron spectroscopy

ABSTRACT

The adsorption of perylene-3,4,9,10-tetracarboxylic-3,4,9,10-diimide (PTCDI) on Au(1 1 1) has been studied using synchrotron-based X-ray photoelectron spectroscopy and in situ scanning tunnelling microscopy. Direct topographic and surface coverage information provided by the scanning probe measurements have enabled us to correlate peaks in the relatively complex carbon core-level photoemission to interactions of the surface with different parts of the PTCDI molecule. A strong interaction between the imide ends of the molecule with the underlying gold substrate is evidenced by a large chemical shift in the imide carbon peaks, which is observed only for the first adsorbed layer.

1. Introduction

Molecular self-assembly for the formation of ordered templates and nanostructures on surfaces relies on a balance between non-covalent intermolecular interactions and the nature of the adsorption to the underlying surface [2,6]. The results can be quite spectacular, with the formation of two-dimensional molecular templates being driven by intermolecular forces such as hydrogen bonding and van der Waals interactions [3,7,23]. One system which exhibits these qualities is that of perylene tetracarboxylic diimide (PTCDI), and its derivatives, combined with melamine on surfaces such as gold and silver-terminated silicon under UHV conditions [11–13,15–19,24]. Even without the co-adsorption of other molecules, perylene derivatives can form a variety of ordered phases and molecular networks on surfaces by virtue of this interplay between surface and molecular interactions [21]. Scanning tunnelling microscopy (STM) shows clearly that PTCDI adsorbs with the molecular plane lying parallel to the surface on Au(1 1 1) forming large hydrogen-bonded islands [5,9] (also PTCDA [10,20]), and the fact that self-assembled equilibrium structures can be formed at temperatures below 100 °C suggests that the interaction with the surface is relatively weak. The bonding of large organic molecules to metal surfaces is often both fascinating and complex. It has generally been found that perylene derivatives are more strongly bound to surfaces such as Ag(1 1 1) [22,25], Ni(1 1 1) [22] and Si(1 1 1) [22], than they are to Au(1 1 1) [25]. Also, that PTCDI interacts more strongly with the former three surfaces than its anhydride analogue PTCDA [22]. In this paper, we explore the chemical nature of the adsorption of PTCDI on the Au(1 1 1) surface by focussing on the carbon 1*s* core-level photoemission spectrum at various coverages, combined with STM measurements performed on identical samples in the same system. In this way, a direct correlation can be made between the arrangement of the molecules on the surface and the features in the core-level photoemission. The results suggest that for the first molecular layer adsorbed on the surface there is a significant interaction between the imide ends of the molecule and the Au(1 1 1) surface which causes a large chemical shift in the core-level peaks associated with the carbon atoms in these groups (see Fig. 1). However, this is not true for all molecules in the first complete monolayer.

2. Method

The experiment was performed at the wiggler beamline MPW 6.1 at Daresbury SRS [4]. Photoemission and scanning tunnelling microscopy (STM) measurements were carried out using two 4 mm × 8 mm 1500 Å gold on mica substrates (Agilent, USA). The samples were prepared in the same chamber under identical conditions and the PTCDI depositions were carried out simultaneously, with one sample subsequently being analysed by STM and the other by photoemission in parallel so as to make full use the synchrotron radiation. Cleaning was carried out by sputtering using 0.7 keV Ar^+ ions, and annealing to ~500 °C. Images of the surface

* Corresponding author. Tel.: +44 0 115 8515149.
E-mail address: james.oshea@nottingham.ac.uk (J.N. O'Shea).

0039-6028/$ - see front matter © 2009 Elsevier B.V. All rights reserved.
doi:10.1016/j.susc.2009.08.024

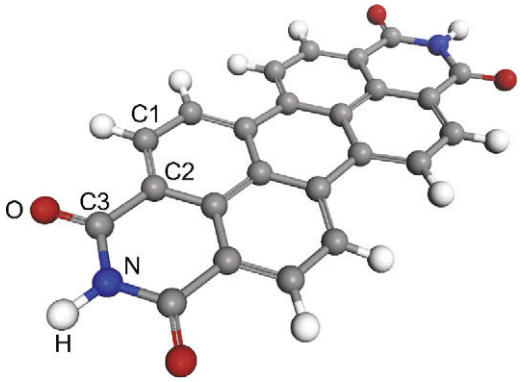

Fig. 1. Schematic representation of the PTCDI molecule. The numbered atoms refer to the chemically different carbon atoms that give rise to resolvable peaks in the core-level photoemission: (C1) carbon atoms along the outside of the perylene core bonded to two carbon atoms and one hydrogen atom, (C2) carbon atoms bonded to three other carbons within the perylene core, and (C3) carbon atoms in the imide end groups.

were acquired using an Omicron scanning tunnelling microscope, housed within the UHV system, using electrochemically etched tungsten tips, and operating in constant current mode at room temperature. The base pressure in the UHV system was 1×10^{-10} mbar. Images of the surface taken after the sputter-anneal cycle show the characteristic $(22 \times \sqrt{3})$ herringbone reconstruction of the Au(1 1 1) surface [1]. PTCDI molecules were sublimed onto the clean surface using a Knudsen-cell evaporator at a temperature of ~360 °C positioned approximately 20 cm from the sample surface. This gave a deposition rate of ~0.1 ML min^{-1} at the surface. Photoemission spectra were measured using a hemispherical analyser. The presented C 1*s* spectra were excited using a photon energy of 340 eV and the binding energy scale calibrated to the Fermi level of the underlying gold substrate. The total instrument resolution measured from the width of the Fermi edge was <145 meV. Values for the surface coverage were obtained from a statistical assessment of the STM images, based on the aerial coverages observed.

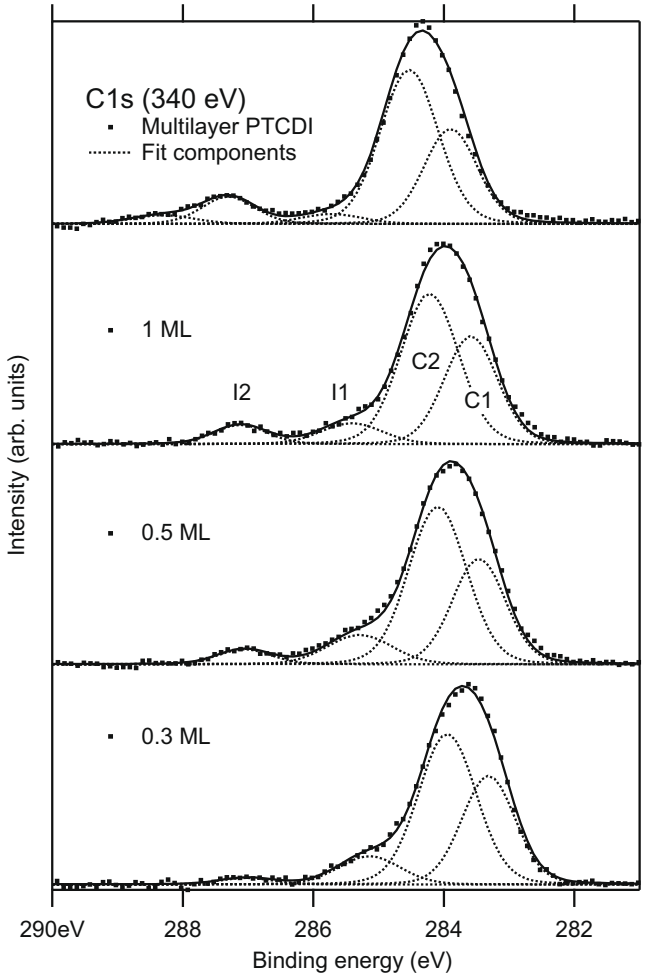

Fig. 2. C 1*s* core-level photoemission spectra measured using $h\nu = 340$ eV for the indicated coverages of PTCDI on the Au(1 1 1) surface (0.3 ± 0.06 ML, 0.5 ± 0.07 ML, 1.0 ± 0.02 ML and multilayer). Total instrument resolution was <145 meV.

3. Results and discussion

The C 1*s* core-level photoelectron spectra for increasing coverage of PTCDI adsorbed on the Au(1 1 1) surface are shown in Fig. 2. The spectra have been fitted using a combination of symmetric Voigt lineshapes (see Table 1) following subtraction of a polynomial background. The main peak at around 284 eV binding energy is asymmetric and arises from the carbon atoms in the perylene core. Here, we have fitted this peak with two components, the lower binding energy component corresponding to the eight C1 carbon atoms shown in Fig. 1 bonded to two other carbons and a hydrogen atom, and the higher binding energy component corresponding to the 12 C2 carbon atoms bonded to three other carbons in the perylene core. These are chemically shifted from one another by 0.6 eV, which is comparable to the shifts reported for the anhydride analogue PTCDA adsorbed on the Ag/Si(1 1 1)$(\sqrt{3} \times \sqrt{3})$ [8] and Ag(1 1 1) surfaces [25]. For the multilayer coverage there is a peak (and associated shake-up) corresponding to the four carbon atoms contained within the two imide end groups of the molecule. This peak, I2 is located at a binding energy 3.4–3.6 eV above C1, depending on the coverage. At the lowest surface coverage (0.3 ML) I2 is barely visible and is instead replaced by the component I1, much closer in energy to the perylene core at a binding energy of 1.8 eV above C1. At intermediate coverages the intensity of the high binding energy imide peak increases smoothly and there is a gradual suppression of the lower binding energy component. For clarity, we have not shown spectra for 0.7 ML and 1.3 ML, which simply continue the trend observed in the presented spectra. The C 1*s* data therefore suggests that at low coverages the interaction of the PTCDI molecule with the Au(1 1 1) surface is dominated by a strong interaction with the imide end groups. The peak I1 is thus assigned to an imide group bonded to the surface, while peak I2 is assigned to a non-interacting imide (note that here we refer only to the interaction with the underlying surface, most imide groups will also take part in a hydrogen-bond interaction with their nearest neighbor). For the multilayer the spectrum in Fig. 2 exhibits a weak shake-up feature at around 288 eV, which is suppressed at lower coverages due to the interaction with the gold surface [14] and was observed only at 1.3 ML and above. It is worth noting that while it would not be feasible to include it in the fit, a corresponding shake-up associated with C2 could also be present for the multilayer, and thus the intensity of the I1 peak at higher coverages may be an overestimate [8].

The large chemical shift observed for the imide carbons interacting with the gold surface suggests the formation of a chemical bond, and therefore that PTCDI is, to some extent at least, chemisorbed to the Au(1 1 1) surface. A similar shift to lower binding energy has previously been observed for the carboxylic groups of the anhydride analogue PTCDA on Ag(1 1 1) [25]. In the case of PTCDA, this shift was observed only for the Ag(1 1 1) and not the Au(1 1 1)

Table 1
Parameters for the C1s spectra (all binding energy and full width at half maximum (FWHM) values in eV).

	0.3 ML	0.5 ML	1.0 ML	Multilayer
Position of ring periphery carbons	283.3	283.5	283.6	283.9
Relative position of aromatic carbons	0.6	0.6	0.6	0.6
Relative position of interacting imide carbon	1.8	1.8	1.8	1.8
Relative position of non-interacting imide carbon	3.6	3.6	3.5	3.4
FWHM of ring periphery carbons	0.9	0.9	0.9	0.9
FWHM of aromatic carbons	1.0	1.0	1.0	1.0
FWHM of interacting imide carbon	1.1	1.1	1.1	1.1
FWHM of non-interacting imide carbon	0.9	0.9	0.9	0.9
Normalized area of ring periphery carbons	0.35	0.35	0.34	0.34
Normalized area of aromatic carbons	0.53	0.50	0.52	0.51
Normalized area of interacting imide carbon	0.10	0.10	0.08	0.04
Normalized area of non-interacting imide carbon	0.02	0.05	0.06	0.12[a]

[a] Non-interacting imide area for multilayer coverage contains the shake-up to higher binding energy.

surface, the conclusion being that the molecule is chemisorbed to the former and physisorbed to the latter. The chemical nature of the imide group of PTCDI however, appears to allow it to chemisorb to the Au(1 1 1) surface in stark contrast to its anhydride counterpart. That PTCDI molecules have sufficient mobility on the surface at elevated temperatures to form self-assembled networks suggests that the diffusion barrier is not insurmountable despite the formation of a chemisorption bond.

The fact that the imide carbon peak in the C 1*s* is very different in the sub-monolayer regime compared to that of the multilayer, while the ring peaks are essentially unchanged, strongly indicates that it is these carbons that are primarily used in chemisorption to the surface. However, as can be seen from Fig. 2 the transition is a smooth one, in that an abrupt shift at 1 ML is not observed. Instead, the appearance of non-interacting imide carbons occurs *before* a nominally full monolayer coverage. This suggests either that second layer growth occurs before the completion of the first monolayer, or that the imide interaction only occurs for specific adsorption sites, which are more readily accessible at lower coverage. In order to address this question STM measurements were carried out on the same samples, by incorporating a scanning tunnelling microscope into the beamline end-station.

Fig. 3 shows STM images representative of those used to calculate the surface coverage of the PTCDI islands adsorbed upon the Au(1 1 1) substrate. The current data for the images is shown here to demonstrate the difference between the clean substrate and the molecular domains, with the images on the left being coloured/shaded to highlight the regions of PTCDI. From these current images it would appear that the onset of second layer growth does not occur until after the completion of a full monolayer. However, a full analysis of the STM data set indicates that a small fraction of molecules (less than 0.05 of a monolayer) are present in 2nd and 3rd monolayer growth at 0.7 ML coverage. Fig. 4b shows an STM image with molecular resolution of multilayer growth taken at a coverage of 0.7 ML; contrasting with the monolayer close-packed structure observed at 0.5 ML in Fig. 4a). Clearly, the changes in the ratio of interacting and non-interacting imide peaks in the C 1*s* photoemission of Fig. 2 cannot be due to the relative abundances of first and second layer molecules. The origin of the chemical shift must instead lie with a specific adsorption site.

We can directly compare the C 1*s* spectra for 0.3 ML and 1.0 ML since we know from the STM images that the amount of second layer growth and therefore any attenuation of the underlying molecules is very low. At 0.3 ML coverage interacting imides make up around 83% of the molecules present, while at 1.0 ML this amounts to only 57%. So while the rate of increase in the amount of interacting imide is slower than for the non-interacting signal, it nevertheless continues to increase until monolayer coverage is exceeded, at which point the interacting imide peak becomes suppressed by subsequently adsorbed layers. Two things become clear. Firstly, that the low binding energy peak associated with the interacting imide is derived from those molecules involved in a direct interaction with the gold surface, and second, that the assignment of the high binding energy peak to a non-interacting imide is confirmed by its presence in the multilayer. It is also important to note that there is not a gradual binding energy shift from one state to the other, both peaks represent distinct bonding states at relatively fixed binding energies. This rules out a gradually decreasing interaction strength with increasing coverage. At very low coverage it is reasonable to expect a substantial fraction of molecules to adsorb preferentially at step edges and defects. However, at coverages higher than 0.3 ML and certainly at 1.0 ML it is not reasonable to expect that more than half of the molecules present can be adsorbed at such sites.

We are left with the unambiguous conclusion that at surface coverages well below a monolayer the vast majority of PTCDI molecules adsorb in a configuration that provides a very strong interaction between the imide groups and the gold surface, most likely due to a charge transfer interaction. At coverages approaching a full monolayer, this is possible only for around half of the imide groups and we thus observe a comparable signal from both interacting and non-interacting imide groups in the C 1*s* photoemission. Unfortunately, while the STM images obtained in this study are sufficient for determining the surface coverage and morphology of PTCDI islands they are unable to provide information about the specific adsorption sites on the Au(1 1 1) surface or the commensurability of the monolayer with the surface lattice. Our STM data also does not reveal whether the ordering in the second layer is exactly the same as that in the first. It is possible that the herringbone reconstruction of the surface plays a significant role in this respect, or even that the reconstruction is lifted by the adsorption of PTCDI molecules, which will be the topic of future investigations. The most likely scenario is that at very low coverage molecules many of the molecules can adopt an adsorption geometry in which both imide groups are chemically bound to the surface. As the coverage increases, steric hindrances allow only a bonding geometry in which one imide group is bound in this way.

4. Conclusions

Combining synchrotron-based photoemission with in situ scanning tunnelling microscopy the C 1*s* core-level spectra can be used to understand the bonding of PTCDI to a Au(1 1 1) surface as a function of coverage. The spectra suggest a strong interaction between the imide end groups of the molecule and the surface, which is reflected in a large chemical shift to lower binding energy of the imide carbon atoms, while the perylene core remains relatively

unperturbed. The presence of both interacting and non-interacting imide groups and the increasing prevalence of the latter as the coverage increases is shown by STM not to be due to second layer growth. In contrast to the anhydride analogue PTCDA, which is

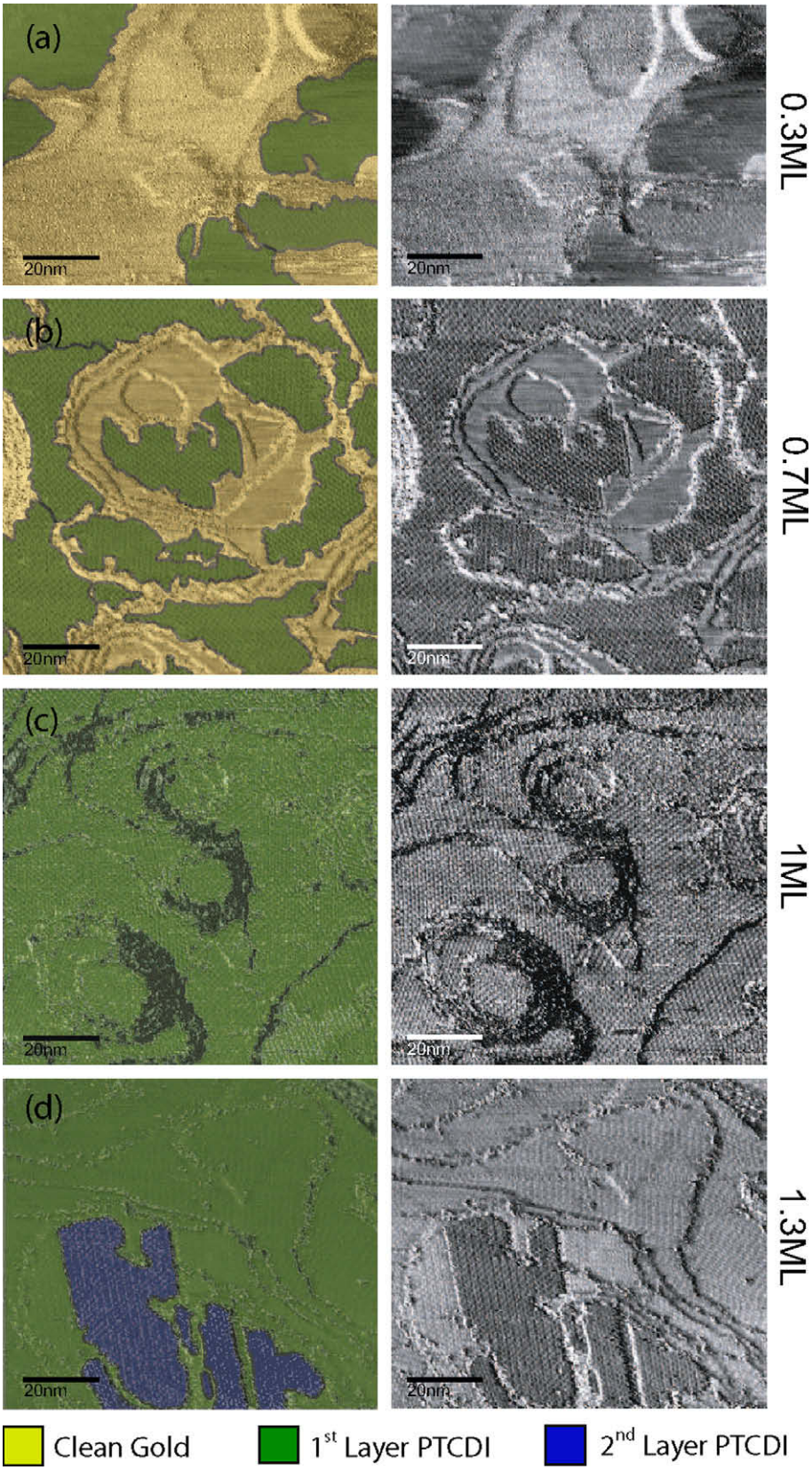

Fig. 3. STM images showing domains of PTCDI adsorbed on Au(1 1 1) for (a) 0.3 ML, (b) 0.7 ML, (c) 1.0 ML, and (d) 1.3 ML coverages. Data presented is of the current signal with the coloured/shaded images on the left highlighting the regions of PTCDI. Images were acquired using a tunnel current of 50 pA and a sample bias of (a) +1.80 V, (b and d) −1.80 V, and (c) +1.50 V. Scale bars are shown on the images.

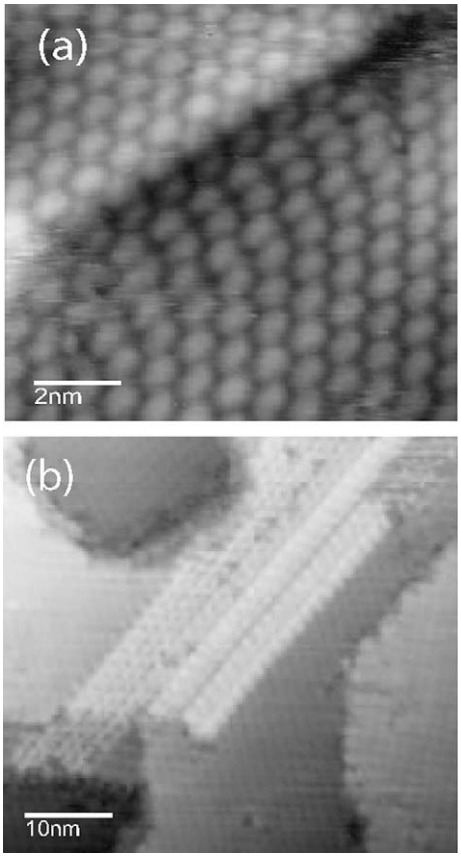

Fig. 4. STM images with molecular resolution of the adsorbed PTCDI islands. Images show (a) the close-packed arrangement for PTCDI which has been observed previously (image taken from 0.5 ML coverage), and (b) the start of 2nd and 3rd layer island growth occurring at 0.7 ML coverage. Images were acquired using a tunnel current of 50 pA and a sample bias of −1.80 V. Scale bars are shown on the images.

physisorbed to Au(1 1 1) and chemisorbed to Ag(1 1 1), the data suggests that PTCDI is capable of forming a very strong chemical or charge transfer interaction with the Au(1 1 1) in very specific adsorption sites. The ability to adopt this adsorption geometry clearly decreases as the coverage approaches a monolayer where the interaction is found for approximately half of the imide groups (this of course could imply one imide from each molecule or both imide groups from half of the molecules, the former being the most likely). This difference must be attributed to the different chemical nature of the imide and anhydride functional groups. The observation of a strong imide interaction with the surface might shed light on the reason why many PTCDI-derived supramolecular networks have a periodicity commensurate with the Au(1 1 1) surface.

Acknowledgements

The authors would like to acknowledge the Engineering and Physical Sciences Research Council (EPSRC) for funding under Grant Nos. GR/R91953/01 and EP/D048761/1, the European Commission through the Early Stage Researcher Training Network MONET, MEST-CT-2005-020908, and the Science and Technology Facilities Council (STFC) for the provision of time at the SRS.

References

[1] J.V. Barth, H. Brune, G. Ertl, R.J. Behm, Phys. Rev. B 42 (1990) 9307.
[2] J.V. Barth, G. Constantini, K. Kern, Nature 437 (2005) 671.
[3] Matthew O. Blunt, James C. Russell, Maria DelCarmen Gimenez-Lopez, Juan P. Garrahan, Xiang Lin, Martin Schroder, Neil R. Champness, Peter H. Beton, Science 322 (2008) 1077.
[4] M. Bowler, J.B. West, F.M. Quinn, D.M.P. Holland, B. Fell, P.A. Hatherly, I. Humphrey, W.R. Flavell, B. Hamilton, Surf. Rev. Lett. 9 (2002) 577.
[5] M.E. Canas-Ventura, W. Xiao, D. Wasserfallen, K. Mullen, H. Brune, J.V. Barth, R. Fasel, Angew. Chem. Int. Ed. 46 (2007) 1814.
[6] Dimas G. de Oteyza, Inaki Silanes, Miguel Ruiz-Oses, Esther Barrena, Bryan P. Doyle, Andres Arnau, Helmut Dosch, Yutaka Wakayama, J. Enrique Ortega, Adv. Func. Mater. 19 (2009) 259–264.
[7] S. De Feyter, F.C. De Schryver, Chem. Soc. Rev. 32 (2003) 139.
[8] J.B. Gustafsson, H.M. Zhang, E. Moons, L.S.O. Johansson, Phys. Rev. B 75 (2007) 155413.
[9] S. Jensen, C.J. Baddeley, J. Phys. Chem. C 112 (2008) 15439.
[10] L. Kilian, E. Umbach, M. Sokolowski, Surf. Sci. 600 (2006) 2633.
[11] R. Madueno, M.T. Raisanen, C. Silien, M. Buck, Nature 454 (2008) 618.
[12] L.M.A. Perdigao, E.W. Perkins, J. Ma, P.A. Staniec, B.L. Rogers, N.R. Champness, P.H. Beton, J. Phys. Chem. B 110 (2006) 12539.
[13] Luis M.A. Perdigao, Alex Saywell, Giselle N. Fontes, Paul A. Staniec, Gudrun Goretzki, Anna G. Phillips, Neil R. Champness, Peter H. Beton, Chem. A Eur. J. 14 (2008) 600.
[14] C.J. Satterley, L.M.A. Perdigao, A. Saywell, G. Magnano, A. Rienzo, L.C. Mayor, V.R. Dhanak, P.H. Beton, J.N. O'Shea, Nanotechnology 18 (2007) 455304.
[15] C. Silien, M.T. Raisanen, M. Buck, Angew. Chem. Int. Ed. 48 (2009) 1.
[16] F. Silly, A.Q. Shaw, G.A.D. Briggs, M.R. Castell, Appl. Phys. Lett. 92 (2008).
[17] F. Silly, A.Q. Shaw, M.R. Castell, G.A.D. Briggs, Chem. Commun. 1907 (2008).
[18] F. Silly, A.Q. Shaw, K. Porfyrakis, G.A.D. Briggs, M.R. Castell, Appl. Phys. Lett. 91 (2007) 253109.
[19] Paul A. Staniec, Luis M.A. Perdigao, Alex Saywell, Neil R. Champness, Peter H. Beton, Chem. Phys. Chem. 8 (2007) 2177.
[20] R. Staub, M. Toerker, T. Fritz, T. Schmitz-Hubsch, F. Sellam, K. Leo, Surf. Sci. 445 (2000) 368.
[21] J.C. Swarbrick, J. Ma, J.A. Theobald, N.S. Oxtoby, J.N. O'Shea, N.R. Champness, P.H. Beton, J. Phys. Chem. B 109 (2005) 12167.
[22] J. Taborski, P. Vaterlein, H. Dietz, U. Zimmermann, E. Umbach, J. Elec. Spec. Relat. Phenom. 75 (1995) 129.
[23] Kazukuni Tahara, Shuhei Furukawa, Hiroshi Uji-i, Tsutomu Uchino, Tomoyuki Ichikawa, Jian Zhang, Wael Mamdouh, Motohiro Sonoda, Frans C. De Schryver, Steven De Feyter, Yoshito Tobe, J. Am. Chem. Soc. 128 (2006) 16613.
[24] J.A. Theobald, N.S. Oxtoby, M.A. Phillips, N.R. Champness, P.H. Beton, Nature 424 (2003) 1029.
[25] Y. Zou, L. Kilian, A. Scholl, T. Schmidt, R. Fink, E. Umbach, Surf. Sci. 600 (2006) 1240.